  Bull. Chem. Soc. Jpn., 63, 2672—2681 (1990)

Salen-Capped Porphyrins as an Active Site Model of Metalloenzymes: Synthesis and Their Intramolecular Interactions between the Metal Complexes

Kazuhiro MARUYAMA,* Fumikazu KOBAYASHI, and Atsuhiro OSUKA
Department of Chemistry, Faculty of Science, Kyoto University, Kyoto 606
(Received May 17, 1990)

Reversible Schiff base condensation of bis(salicylaldehyde)-linked porphyrins and ethylenediamine under high dilution gave salen-capped porphyrins in high yields. Site selective insertion of nickel(II) into the salen and zinc(II) into the porphyrin gave the corresponding Ni-Zn heterobinuclear complexes. The geometrical relationship between the two metal centers was estimated by ^{1}H NMR spectroscopy. The porphyrin π electronic state of these Ni-salen-capped Zn-porphyrins was perturbed by their Ni-salen cap, which was studied by 400 MHz ^{1}H NMR, UV-Vis spectra, fluorescence, and cyclic voltammetry measurements.

In the last decade, extensive studies of binuclear metal complexes have been made as simple chemical models for biological metalloproteins containing bimetallic centers.[1] One of the important requirements for the model complexes is the close proximity of two metal centers in a well-defined three dimensional geometry, as is found in biological systems. Key roles of the hemoproteins and porphyrin pigments in biological systems provide impetus for the construction of porphyrin dimers[2] and other binucleating porphyrins.[3,4] Porphyrin dimers have been extensively studied as models for the 'special pair' in the photosynthetic reaction center and as donor-acceptor type substrates for intramolecular electron-transfer reactions and excitation energy transfer reactions, while heterobinucleating porphyrin ligands have attracted considerable attention in view of the construction of synthetic receptor molecules[3] and synthetic enzyme models for bimetallic hemoproteins such as cytochrome oxidase.[4] In this paper, we describe the synthesis and physical properties of salen (*N,N'*-disalicylideneethylenediamine)-capped porphyrins.[5] Since the salen ligands are widely known to form stable complexes with a variety of transition metals, the salen-porphyrin binucleating ligand system are useful as a model for studying the interactions of the metalloporphyrins with other transition metal complexes. We synthesized three salen-capped porphyrins (**1**—**3**) with different orientations: A parallel orientation for **1** and **2** and a perpendicular one for **3**, so as to estimate the geometric effects on their interactions between the two metal sites.

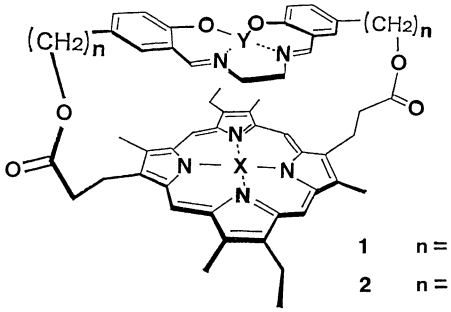

1 n = 2
2 n = 3

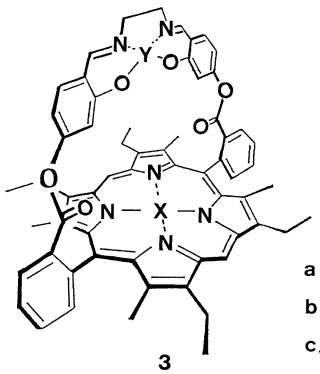

3
a, X = Y = H_2
b, X = H_2, Y = Ni
c, X = Zn, Y = H_2
d, X = Zn, Y = Ni

Results and Discussion

Synthesis of Salen-Capped Porphyrins. Our synthetic route to salen-capped porphyrins utilized the Schiff base condensation of bis(salicylaldehyde)-linked porphyrins (**4**—**6**) with ethylenediamine in the final step.

Salen-capped porphyrins **1a** and **2a** were prepared from mesoporphyrin II dimethyl ester (**7**)[6] as follows: — The dimethyl ester **7** was hydrolyzed under acidic conditions to mesoporphyrin II (**8**),[6] which was transformed into the bis(acid chloride) **9**[7] and then reacted with 2-hydroxy-5-(2-hydroxyethyl)benzaldehyde (**10**) and 2-hydroxy-5-(3-hydroxypropyl)benzaldehyde (**11**) to give bis(salicylaldehyde) linked porphyrins **4** and **5** in 76% and 72% yields, respectivelly.(Scheme 1)

The aldehydes **10** and **11** were obtained as follows: — Commercially available 4-hydroxyphenethyl alcohol (**12**) was treated with acetyl chloride in CH_2Cl_2 to protect the alcoholic hydroxyl group, and then the formyl group was introduced at the 3-position by HCHO/$SnCl_4$ method.[8] Hydrolysis under acidic conditions gave the aldehyde **10** in overall 45% yield. (Scheme 2) Similarly, the aldehyde **11** was prepared from 3-(4-hydroxyphenyl)-1-propanol (**13**) in overall

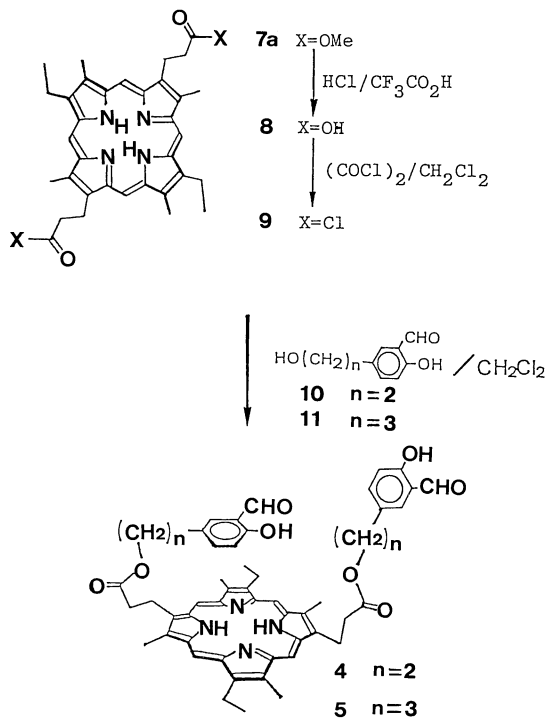

Scheme 1.

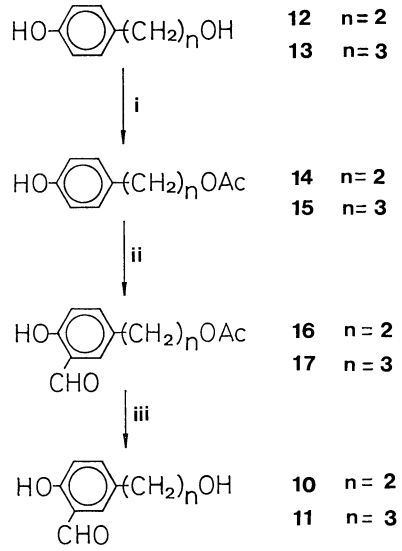

Scheme 2. Reagents: i, AcCl/CH_2Cl_2; ii, $SnCl_4$, triethylamine/toluene then paraformaldehyde; iii, 4M HCl–THF.

33% yield.

The bis(salicylaldehyde)-linked porphyrin **4** reacted with an equimolar amount of ethylenediamine under high dilution ($<3\times10^{-4}$ M, 1 M=1 mol dm^{-3}) for a prolonged period of time (1—2 weeks). Schiff base formation was monitored by TLC (silica gel, CH_2Cl_2–10% ether). At an early stage of the reaction, intermediate condensation products (presumably **18a**,

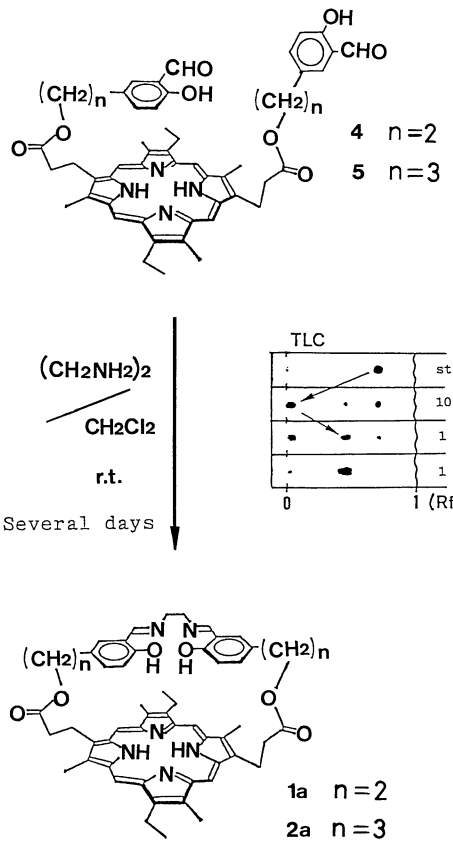

Scheme 3.

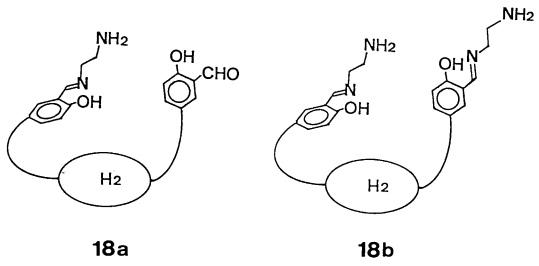

18b), which eluted very slowly on TLC (R_f <0.1), rapidly appeared. But on prolonged reaction, these polar products disappeared slowly and instead the salen-capped porphyrin **1a** (R_f=0.4—0.5) steadily accumulated. After 1 week, almost all of the original porphyrin **4** was converted to **1a**. Evaporation of the solvent followed by addition of methanol induced nearly complete precipitation of the salen-capped porphyrin **1a** in 70% yield. Similarly, the bis(salicylaldehyde)-linked porphyrin **5** was converted to the salen-capped porphyrin **2a** in 81% yield. Many macrocyclizations use irreversible reactions, and the product yield is often unsatisfactory. On the other hand, the Schiff base condensation is reversible attaining an equilibrium on prolonged reaction time, where the capped porphyrin is entropically favored over the linear condensation products under the high

dilution conditions ($<3\times10^{-4}$ M).[9]

A salen-capped porphyrin (**3a**) with perpendicular orientation was synthesized from the bis(salicylaldehyde)-linked porphyrin **6a**, which was prepared from 5,15-bis(2-methoxycarbonylphenyl)etioporphyrin II (**19**) as shown in Scheme 4. 5,15-Bis(2-methoxycarbonylphenyl)etioporphyrin II(**19**) was prepared by the modified Gunter's method.[4a,10] The dimethyl ester **19** was hydrolyzed under basic conditions to give the porphyrin diacid **20**, which consisted of α,α- and α,β-isomers in a ratio of ca. 1:1. This mixture was converted into acid chloride without separation and the acid chloride thus prepared was treated with 2,4-dihydroxybenzaldehyde. Although 2,4-dihydroxybenzaldehyde is itself insoluble in dichloromethane, addition of an equimolar amount of pyridine solubilized it in dichloromethane, so that reaction with the acid chloride **20** (selectively at the 4-hydroxyl group) gave the bis(salicylaldehyde)-linked porphyrin **6a** in 83% yield ($\alpha,\alpha/\alpha,\beta$=1/3 from ^{1}H NMR). At this stage, two stereoisomers were separated by flash column chromatography. We assigned the more polar compound (which moved more slowly on silica gel TLC) as the isomer of α,α-configuration (**6a**: α,α). This isomer was treated with ethylenediamine to give the salen-capped porphyrin (**3a**) in 75% yield, and our assignment was unambiguously confirmed.

The α,β-isomer (**6a**: α,β) was converted to the zinc complex and refluxed in *o*-dichlorobenzene to give the atropisomeric mixture, which was again separated by flash column chromatography.[4a] The zinc complex of the α,α-isomer (**6c**: α,α) reacted with ethylenediamine to give the salen-capped porphyrin **3c** in 80% yield.

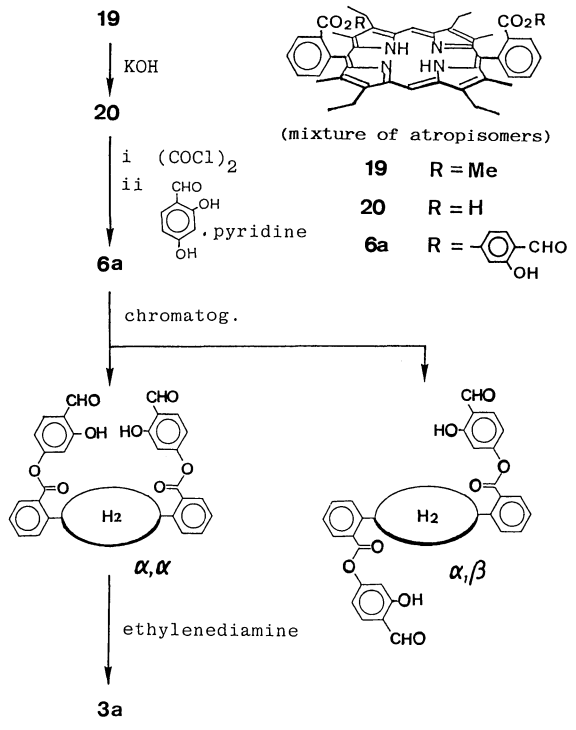

Scheme 4.

Synthesis of Hetero-Binuclear Metal Complexes. For the preparation of hetero-metal complexes, the difference in affinity between the salen and the porphyrin ligands was utilized. Thus, treatment of the salen-porphyrin ligands with nickel(II) acetate in dichlormethane at room temperature resulted in the insertion of nickel(II) into the salen site only even with excess nickel acetate, but in refluxing chloroform, both sites were metallated to give the corresponding bis-nickel complexes. In contrast, zinc(II) was selectively inserted to the porphyrin site on treatment with zinc(II) acetate in dichloromethane at room temperature. These phenomena may be ascribed to the intrinsically strong affinity of the salen ligand for the nickel(II) ion and that of the porphyrin ligand for the zinc(II) ion. Usually, after the insertion of nickel(II) into the salen site, the porphyrin site was metallated with zinc(II) acetate to give nickel-salen-zinc-porphyrin complexes in nearly quantitative yields.

^{1}H NMR and the Geometries of Salen-Capped Porphyrins. The ^{1}H NMR spectra of salen-capped porphyrins (**1a**, **1d**, and **2d**) illustrate many of the features characteristic of the capped structure.[11] (Fig. 1) The propionate side-chain protons appeared in the normal region but as four complex multiplets (each of 2H, a,a',b,b' in Fig. 1) due to restricted conformations. The salen-cap protons were upfield shifted up to about 2 ppm from their usual chemical shift (e,e' in Figure 1) by the strong diamagnetic shielding effect of porphyrin ring current, indicating that the salen units were forced to be held above the porphyrin plane.

Other salen-capped porphyrins also showed upfield shift for the salen protons (Table 1), but the propionate side-chain protons of **2a** showed simple

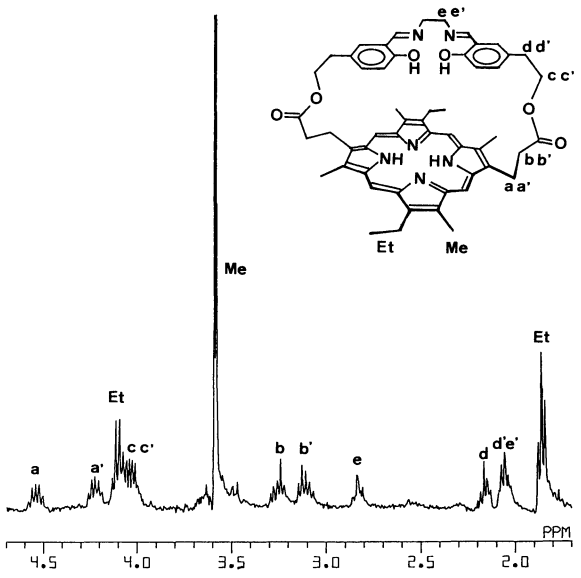

Fig. 1. Partial 400 MHz ^{1}H NMR spectrum of salen-capped porphyrin **1a** in $CDCl_3$.

Table 1. ^{1}H NMR Chemical Shift of Selected Protons in Salen-Capped Porphyrins in $CDCl_3$

Compd	Chemical shift δ/ppm					
	H_a	H_b	H_b'	H_c	H_d	H_e
1a	6.31	6.35	—	5.39	6.25	2.84, 2.06
2a	5.95	5.65	—	5.84	7.21	3.27
3a	5.67	—	4.16	5.71	7.26	3.42
3c	5.03	—	4.77	5.94	7.32	3.37
H_2-Salen	6.94	7.29	6.85	7.22	8.36	3.94
1b	(7.09	6.87	—	6.39)	a)	−1.42, −1.72
2b	a)	a)	—	a)	a)	a)
3b	(5.76	—	5.76	4.56	3.87)	−1.38
1d	(6.71	6.20	—	5.80)	a)	a)
2d	5.78	5.88	—	4.67	5.52	2.54
3d	4.84	—	(5.99	5.76)	7.26	3.8
Ni-Salen	7.04	7.20	6.53	7.06	7.49	3.43

a) Not characterized.

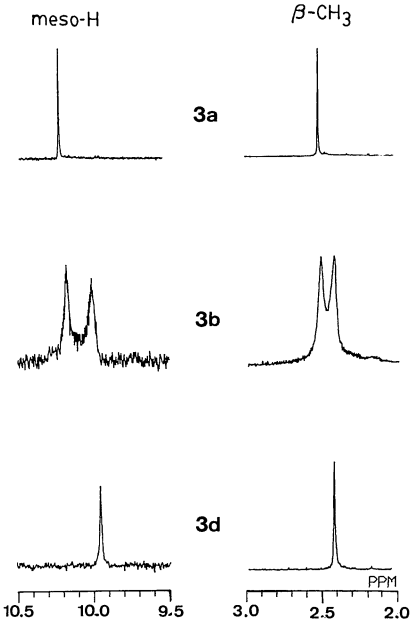

Fig. 2. Resonances of the *meso* protons and β-CH_3 protons of salen-capped porphyrins **3a**, **3b**, and **3d**.

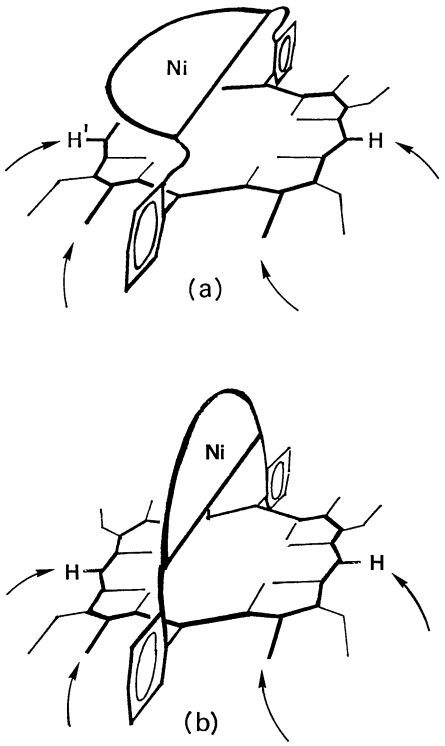

Fig. 3. Proposed conformations for **3b** (a), and **3d** (b).

patterns, indicating the more flexible conformations of longer alkyl chains. In the metal free form, the salen ligand acts like a flexible methylene chain, while rigid square planar structure of the nickel-salen[12] reduces this flexibility, leading to the complicated patterns of the ^{1}H NMR signals. In the case of the mono-nickel complexes **1b** and **2b**, we observed broadened ^{1}H NMR spectra presumably because of the intimate association of the free base porphyrin with the nickel-salen moiety. Strong interactions between the nickel-salen and the free-base porphyrin were also observed in **3b**. The ^{1}H NMR spectrum of **3b** showed two sets of signals in equal intensity (Fig. 2) for *meso*-H and β-CH_3 of the porphyrin (indicated by arrows in Fig. 3), and the methylene protons of the salen (H_e in Table 1) were upfield shifted in a similar magnitude with **1b**, indicating that **3b** was forced to be in a distorted conformation and thus two meso protons and peripheral methyl protons were not equivalent[13] (Fig. 3a). In contrast, it is noteworthy that the corresponding nickel-salen zinc-porphyrin complex **3d** exhibited single resonances at 9.94 ppm for *meso*-H and at 2.41 ppm for β-CH_3 and the upfield shift of H_e was not observed, indicating either that the Ni-salen-cap was in a perpendicular arrangement relative to the porphyrin or that it was undergoing of flapping motion which was faster than the time scale of the ^{1}H NMR measurement (Fig. 3b).

Time-averaged conformations of the nickel-salen-capped zinc-porphyrins **1d**, **2d**, and **3d** can be deduced from their 400 MHz ^{1}H NMR spectra by analyzing porphyrin-ring-current induced chemical shift changes.[14] Protons of the nickel-salen-cap were up-field shifted relative to the unsubstituted nickel-salen due to the porphyrin ring current, indicating that the salen moieties were above the porphyrin plane in each cases (Table 1).

The nickel-salen protons of **1d** were upfield shifted by 0.3—1.2 ppm, while much larger upfield shifts were observed for **2d**. Since the size of the nickel-salen is comparable to the porphyrin, the peripheral protons of the nickel-salen in **1d** protrude out of the porphyrin ring current due to insufficient length of the methylene linkage. This could give rise to a decrease of the ring current shifts. On the other hand, there exist some conformational flexibilities in **2d**, which allow the nickel-salen-cap to take a folded conformation just above the porphyrin ring. Thus the nickel-salen protons in **2d** were all upfield shifted by 1—2 ppm, which seemed to be consistent with a time-averaged face-to-face geometry with 5—6 Å separation, as shown in Fig. 4a. In sharp contrast, the H_d and H_e protons in **3d** did not exhibit up-field shifts and the H_a protons were markedly upfield shifted, suggesting a nearly perpendicular arrangement of the nickel-salen-cap to the porphyrin ring. (Fig. 4b) Metal-metal distance and edge-to-edge distance between the nickel-salen and the zinc-porphyrin of **3d** were estimated to be 7.0—7.5 Å and 5 Å, respectively, on the basis of the porphyrin ring current model.[14] These geometric arrangements were supported by Corey–Pauling–Koltun (CPK) molecular models, which gave estimated metal–metal distances to be 4.8 Å in **1d**, 5.6 Å in **2d**, and 7.2 Å in **3d**, respectively; in good agreement with those estimated from ring-current shifts.

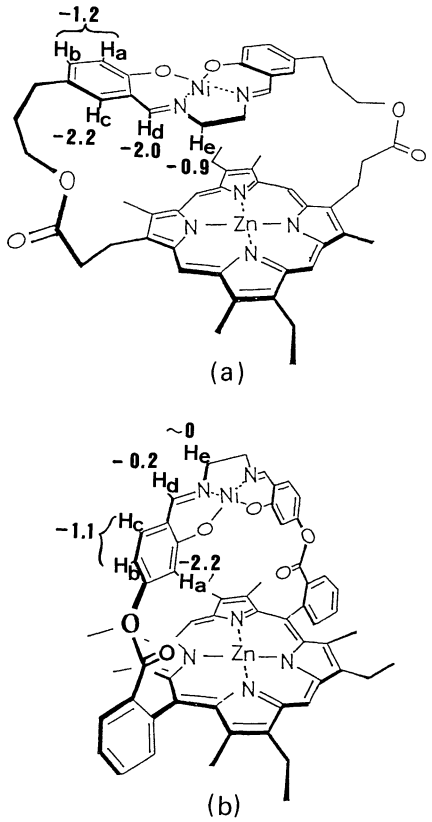

Fig. 4. Observed upfield ring-current shifts (negative values in ppm) with resprct to nickel-salen in the ^{1}H NMR spectra ($CDCl_3$) and proposed conformations of **2d** and **3d**.

Absorption Spectra snd Electrochemistry. The absorption spectra of the nickel-salen-capped porphyrins contained Soret and Q-bands due to the porphyrin as well as the nickel-salen absorption in UV region (λ_{max} 250 nm). Though the shapes of Soret and Q-bands of **1b** and **2b** were almost unchanged relative to **7a**, both Soret and Q-bands were ca. 3—4 nm red-shifted by the nickel-salen-cap (Table 2). In the nickel-salen-capped

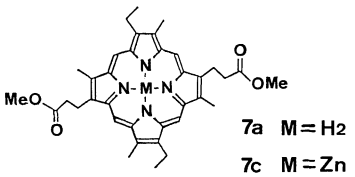

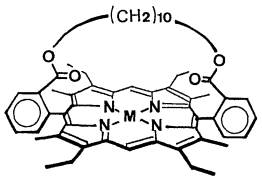

Table 2. UV-Vis Spectral Data[a]

Compd	λ_{max}/nm	
	Soret	Q-bands
1a	400	498, 534, 568, 621
2a	400	499, 533, 567, 621
1b	403	504, 538, 568, 621
2b	402	502, 536, 569, 624
7a	398	498, 533, 566, 620
3a	412	508, 541, 577, 625, 656
3b	406	506, 539, 572, 624, 654
21a	410	507, 540, 576, 629, 654
1d	410	538, 574
2d	404	535, 571
7c	401	531, 568
3c	417	543, 583
3d	418	548, 583
21c	412	540, 575

a) Measured in CH_2Cl_2 solution.

zinc-porphyrins **1d**, **2d**, and **3d**, Soret and Q-bands of the porphyrin were substantially red-shifted (Table 2). Compound **1d**, especially showed 9 nm red shift of the Soret band together with some broadening, compared with **7c**, suggesting strong ground state interactions between the macrocycle and the Ni-salen-cap. As a unique case, **3b** showed a 4 nm blue shift compared with **21a**, which should be ascribed to the distorted conformations of **3b** (Fig. 3a). Reversible one-electron oxidation potentials of **1d**, **2d**, and **3d** were much lower than those of the reference porphyrins **7c** and **21c** (Table 3). As proved by ESR measurements,[15] the first oxidation of these nickel-salen-zinc-porphyrin complexes leads to the formation of the corresponding porphyrin π cation radical with the *g*-value of 2.002 which is the same as the π cation radical of zinc-meso-porphyrin II dimethyl ester (**7c**). Although their hyperfine structures are not clear, slightly broadened signals of **1d** and **2d** indicates the perturbation by nickel-salen moieties. (Fig. 5, Table 3) Such broadening of ESR signal was not observed in **3d**.

Since it has been well-established that porphyrins generally show red-shifted Soret bands and lower oxidation potentials in electron-donating solvents or with electron-donating axial ligands,[16] these spectral red shifts and low oxidation potentials of **1d**, **2d**, and **3d** can be ascribed to electron donation from the nickel(II)-salen to the zinc-porphyrin in the ground state.

Table 3.

Compd	$E^{ox}_{1/2}$ a)	$\Delta E^{ox}_{1/2}$	*g*-value d)	ΔH_{pp}/G e)
1d	0.03	−0.16 b)	2.002	4.8
2d	0.05	−0.14 b)	2.002	4.9
7c	0.19	—	2.002	4.2
3d	0.07	−0.08 c)	2.002	3.9
21c	0.15	—	2.002	3.9

a) Oxidation potentials (V vs. ferrocene/ferrocenium, +0.45 V vs. SCE) were measured by cyclic voltammetry at a Pt electrode, in dichloromethane containing 0.1 M (1 M=1 mol dm^{-3}) tetrabutylammonium perchlorate at 20 °C; accuracy±0.01 V. b) Oxidation potential changes with respect to **7c**. c) Oxidation potential change with respect to **21c**. d) ESR *g*-values of one-electron oxidation products. e) Peak to peak line width (±0.2 G).

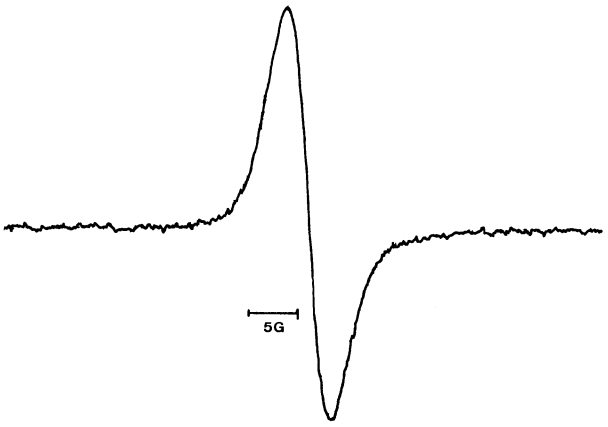

Fig. 5. ESR spectrum of the cation radical derived from **1d**, generated by electrooxidation in CH_2Cl_2.

Fluorescence Quenching. Porphyrin fluorescence was effectively quenched by nickel-salen moiety in **1d**, **2d**, and **3d**. The fluorescence intensities of **1d** and **2d** were 0.02 and 0.04 compared with that of parent porphyrin **7c**, and the fluorescence intensity of **3d** was reduced to 0.10 with respect to reference porphyrin **21c** (Table 4). Picosecond time-resolved fluorescence spectroscopy revealed that the major fraction of the fluorescence of **1d**, **2d**, and **3d** decayed rapidly with fluorescence lifetime of 0.1 ns, 0.15 ns, and 0.3 ns, respectively (Table 4).[17] Fluorescence lifetime of **3d** is 2—3 times longer than those of **1d** and **2d**. We also examined picosecond time-resolved spectra of **1d**.[18] The spectrum at the delay time of 33 ps was almost due to the $S_n \leftarrow S_1$ transition of the Zn-porphyrin. A rapid decay of the $S_n \leftarrow S_1$ absorption at 460 nm was observed and the time constant of the decay (0.14 ns) agreed satisfactorily with the fluorescence lifetime of **1d**. Upon further increase of the delay time to 1 and 5 ns, the $T_n \leftarrow T_1$ absorption at 450 nm was observed, but its

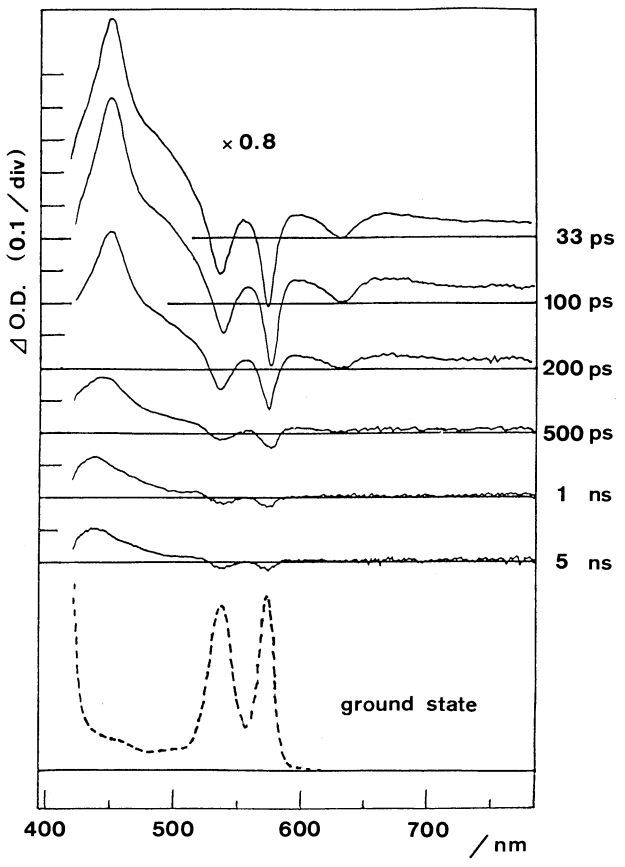

Fig. 6. Picosecond time-resolved transient absorption spectra of **1d** in DMF, excited at 532 nm pulse.

Table 4. Fluorescence Spectral Data[a)]

Compd	λ_{em}/nm	$\Phi_{f,rel}$[b)]	τ/ns[e)]
1d	569, 622	0.02[c)]	0.108 (88%) 0.710 (12%)
2d	571, 622	0.04[c)]	0.153 (85%) 0.854 (15%)
7c	570, 620	1.0	1.45 (100%)
3d	584, 640	0.10[d)]	0.312 (87%) 1.63 (13%)
21c	580, 635	1.0	1.61 (100%)

a) Measured in CH_2Cl_2 solution. b) Relative fluorescence intensities of Q (00) bands; excitation at Soret wavelength. c) With respect to **7c**. d) With respect to **21c**. e) Fluorescence lifetime measured by time-correlated single photon counting;[17] excited at 514.5 nm by Ar laser pulse. Numbers in parentheses indicate the normalized pre-expotential factor.

intensity was not enhanced, indicating that the intersystem crossing of the singlet excited state of zinc-porphyrin was not accelerated by the Ni-salen. Although it was difficult to detect clearly the ion pair state presumably due to its rapid charge recombination, the electron transfer mechanism was expected to play a predominant role for the fluorescence quenching.

As discussed above, **3d** seems to have a nearly perpendicular arrangement of two chromophores, while **1d** and **2d** have a time-averaged face-to-face arrangement. Although the metal–metal distances of **1d** (4.8 Å) and **2d** (5.6 Å) were shorter than those of **3d** (7.2 Å), the edge-to-edge distance between the nickel-salen and the zinc-porphyrin was almost the same for **1d**, **2d**, and **3d** (ca. 5 Å). It is reasonable to consider that an electron-donating interacition from nickel(II)-salen to the porphyrin π-electronic system is mainly orientation-dependent, since electron-filled dz^2 orbital of nickel(II) has an axial direction with respect to the salen-ligand plane. Thus face-to-face geometry between the nickel-salen and the zinc-porphyrin seems more favorable for this electron-donating and other orbital interactions.

In summary, intramolecular macrocyclization reactions produced several novel binucleating salen-capped porphyrins, from which the nickel(II)-zinc(II) hybrid complexes were obtained by selective metallation procedure. In these molecules, the interactions between two metal centers were found to be orientation-dependent: Fluorescence lifetime of **1d** with parallel orientation was 0.1 ns, while 3 times longer lifetime (0.3 ns) was observed in **3d** with perpendicular orientation. Such orientation effects, which can be anticipated in the interactions between geometry-restricted anisotropic molecules, should play important roles in biological systems. Our model systems appear to show properties with a direct bearing on this issue.

Experimental

The ^1H NMR spectra were recorded at 400 MHz on a JEOL JNM-GX-400 spectrometer, with tetrametylsilane or $CHCl_3$ as internal reference. All spectra were measured in $CDCl_3$ solution. High-resolution mass spectra were obtained on a JEOL JMS-DX-300 instrument (3 eV). Fast atom bombardment mass spectra of porphyrins were recorded on a JEOL JMS-HX-110 (10 eV) or a JEOL JMS-DX-300 (1.5 eV) with *m*-nitrobenzyl alcohol as the matrix. UV-Vis spectra were recorded in dichloromethane on a Shimadzu UV-200 and a Shimadzu UV-3000. Steady-state fluorescence spectra were recorded by using a Shimadzu RF-502a. Fluorescence lifetimes were measured by picosecond time-correlated single photon counting technique.[17] ESR measurements were done on a JEOL-JES-FEIXG. Cyclic Voltammetry was performed with a PAR Model 174. The picosecond transient absorption measurements were done by means of a microcomputer-controlled double-beam ps spectrometer with a repetitive mode-locked Nd^{3+}/YAG laser as the excitation source.[18] Flash column chromatography was carried out using Merck Kieselgel 60H Art. 7736 or Merck Kieselgel 60HF254 Art. 7739.

Anhydrous dichloromethane (CH_2Cl_2) was distilled from phosphorus pentaoxide prior to use. Anhydrous toluene was distilled from sodium metal and stored over sodium wire. Anhydrous pyridine was distilled and stored with Molecular Sieves 4A. Triethylamine was distilled and stored over potassium hydroxide.

Unless otherewise stated all reactions were performed under an atmosphere of dry nitrogen. All organic extracts were dried over anhydrous sodium sulfate.

4-Hydroxyphenethyl Acetate (14). 4-Hydroxyphenethyl alcohol (**12**) (5.56 g, 40.2 mmol) was suspended in CH_2Cl_2 (130 ml). Acetyl chloride (4.0 ml) was added and the mixture was stirred at room temperature overnight to give clear solution. After the solvent and excess acetyl chloride were evaporated, the residue was taken up in a little CH_2Cl_2 and filtered through silica gel. Evaporation of the solvent left colorless oil (6.36 g, 35.3 mmol, 88%). ^1H NMR ($CDCl_3$) δ=7.0+6.7 (each 2H, d+d, Ar-H), 6.0 (1H, br, OH), 4.2 (2H, t, CH_2OAc), 2.8 (2H, t, $ArCH_2$), 2.0 (3H, s, CH_3CO).

3-(4-Hydroxyphenyl)propyl Acetate (15). 3-(4-Hydroxyphenyl)-1-propanol (**13**) (2.66 g, 17.5 mmol) was treated with acetyl chloride (1.5 ml) as described above to give colorless oil (2.58 g, 13.3 mmol, 76%). ^1H NMR ($CDCl_3$) δ=7.18+6.90 (2H+2H, d+d, ArH), 4.16 (2H, t, CH_2OAc), 2.70 (2H, t, $ArCH_2$), 2.09 (3H, s, CH_3CO), 1.9 (2H, m, $CH_2CH_2CH_2O$).

2-(3-Formyl-4-hydroxyphenyl)ethyl Acetate (16).[8] 4-Hydroxyphenethyl acetate (**14**) (6.36 g, 35.3 mmol) was dissolved in dry toluene (80 ml). $SnCl_4$ (2 M solution in CH_2Cl_2, 2.6 ml) and triethylamine (2.6 ml) were added. The mixture was stirred for 20 min at room temperature, then paraformaldehyde (2.5 g) was added. The resulting yellowish solution was heated at 100 °C for 8 h. After cooling, the reaction mixture was poured into water (200 ml), acidified with 1 M hydrochloric acid, and extracted with ether. The ether extracts were washed with water and concentrated, and the residue was chromatographed on silica gel eluted with CH_2Cl_2 to give pale yellow oil (4.16 g, 20.0 mmol, 57%). ^1H NMR ($CDCl_3$) δ=10.88 (1H, s, ArOH), 9.86 (1H, s, CHO), 7.38+7.36+6.93 (each 1H, s+d+d, ArH),

4.25 (2H, t, CH_2OAc), 2.91 (2H, t, $ArCH_2$), 2.02 (3H, s, CH_3CO).

3-(3-Formyl-4-hydroxyphenyl)propyl Acetate (17). From 3-(4-hydroxyphenyl)propyl acetate (**15**) (2.58 g, 13.3 mmol), the title compound was synthesized by the same procedure as described above. Pale yellow oil (1.50 g, 6.75 mmol, 51%). ^1H NMR ($CDCl_3$) δ=10.98 (1H, s, ArOH), 10.04 (1H, s, CHO), 7.44+7.00 (2H+1H, m+d, ArH), 4.13 (2H, t, CH_2OAc), 2.68 (2H, t, $ArCH_2$), 2.08 (3H, s, CH_3CO), 1.96 (2H, m, $CH_2C\underline{H}_2CH_2O$).

2-Hydroxy-5-(2-hydroxyethyl)benzaldehyde (10). 2-(3-Formyl-4-hydroxyphenyl)ethyl acetate (**16**) (0.379 g, 1.82 mmol) was dissolved in tetrahydrofuran (THF, 10 ml) and stirred with 4 M hydrochloric acid (10 ml) at room temperature for 2 days. THF was removed and aldehyde was extracted with CH_2Cl_2. Title compound was chromatographically purified on silica gel eluted with CH_2Cl_2. Colorless oil (0.273 g, 1.64 mmol, 90%). ^1H NMR ($CDCl_3$) δ=10.89 (1H, s, ArOH), 9.87 (1H, s, CHO), 7.43+7.39+6.95 (each 1H, s+d+d, Ar-H), 3.87 (2H, t, CH_2OH), 2.86 (2H, t, $ArCH_2$). Found: *m/z* 166.0630. Calcd for $C_9H_{10}O_3$: M, 166.0630.

2-Hydroxy-5-(3-hydroxypropyl)benzaldehyde (11). 2-(3-Formyl-4-hydroxyphenyl)propyl acetate (**17**) (1.50 g, 6.75 mmol) was hydrolyzed as described above to give pale yellow oil (1.02 g, 5.66 mmol, 84%). ^1H NMR ($CDCl_3$) δ=11.02 (1H, s, ArOH), 10.04 (1H, s, CHO), 7.4+7.0 (2H+1H, m+d, ArH), 3.72 (2H, t, CH_2OH), 2.76 (2H, t, $ArCH_2$), 1.9 (2H, m, $CH_2C\underline{H}_2CH_2O$). Found: *m/z* 180.0794. Calcd for $C_{10}H_{12}O$: M, 180.0786.

Mesoporphyrin II Bis[2-(3-formyl-4-hydroxyphenyl)ethyl]-Ester (4). Mesoporphyrin II (**8**)[6] (0.422 g, 0.744 mmol) was dispersed in dry CH_2Cl_2 (90 ml). Oxalyl dichloride (3.0 ml) was added and the mixture was stirred in the dark for 2 h. The solvent and excess oxalyl dichloride were removed under reduced pressure to yield mesoporphyrin II bis(acid chloride) (**9**) as a purple gum.[7] This was dissolved in dry CH_2Cl_2 (100 ml), and a solution of the **10** (0.65 g, 3.9 mmol) in dry CH_2Cl_2 (30 ml) was added with stirring. Stirring was continued for 3 days at room temperature. The mixture was poured into water, and organic layer was washed twice with water, dried over Na_2SO_4, and then evaporated. The residue was flash chromatographed on silica gel eluted with CH_2Cl_2–10% ether. The first band eluted was the desired porphyrin **4**. Recrystallization from CH_2Cl_2–methanol gave purple microcrystals (485 mg, 0.56 mmol, 76%). ^1H NMR ($CDCl_3$) δ=10.6 (2H, br, OH), 10.09+10.07 (each 2H, s+s, *meso*-H), 9.17 (2H, s, CHO), 6.86+6.62+6.52 (each 2H, dd+d+d, ArH), 4.38 (4H, t, β-$C\underline{H}_2CH_2CO$), 4.14 (8H, m, β-$C\underline{H}_2CH_3$, $OC\underline{H}_2CH_2$), 3.66+3.62 (6H+6H, s+s, β-CH_3), 3.24 (4H, t, β-$CH_2C\underline{H}_2CO$), 2.37 (4H, t, $OCH_2C\underline{H}_2Ar$), 1.87 (6H, t, β-$CH_2C\underline{H}_3$), −3.78 (2H, br, NH). IR(KBr) 1730 and 1655 cm^{-1} (C=O). MS(FAB) *m/z* 863(M+H$^+$). Found: C, 71.81; H, 6.30; N, 6.09%. Calcd for $C_{52}H_{54}N_4O$: C, 72.37; H,6.31; N, 6.49%.

Mesoporphyrin II Bis[3-(3-formyl-4-hydroxyphenyl)-propyl] Ester (5). By the same procedure, mesoporphyrin II (**8**) (46.1 mg, 0.081 mmol) was allowed to react with oxalyl dichloride (0.3 ml) and then with the aldehyde **11** (110 mg, 0.61 mmol) to give the title porphyrin **5** as purple crystals (53.1 mg, 0.059 mmol, 72%). ^1H NMR ($CDCl_3$) δ=10.48 (2H, s, OH), 10.06+10.03 (2H+2H, s+s, *meso*-H), 8.64 (2H, s, CHO), 6.27+6.17+5.70 (each 2H, dd+d+d, ArH), 4.43 (4H, t, β-$C\underline{H}_2CH_2CO$), 4.07 (4H, m, β-$C\underline{H}_2CH_3$), 3.92 (4H, t, $OC\underline{H}_2CH_2CH_2$), 3.65+3.63 (6H+6H, s+s, β-CH_3), 3.31 (4H, t, β-$CH_2C\underline{H}_2CO$), 1.83 (6H, t, β-$CH_2C\underline{H}_3$), 1.38 (4H, t, $OCH_2CH_2C\underline{H}_2$), 1.24 (4H, m, $OCH_2C\underline{H}_2CH_2$), −3.91 (2H, br, NH). IR(KBr) 1730 and 1655 cm^{-1} (C=O). MS(FAB) *m/z* 891(M+H$^+$).

2,2′-[Ethylenebis[(nitrilomethylidyne)(4-hydroxy-3,1-phenylene)]bis[ethanol]Diester of Mesoporphyrin II (Salen-Capped Porphyrin 1a, SCP-2-H$_4$). The bis(salicylaldehyde)-liked porphyrin **14** (13.8 mg, 0.016 mmol) was dissolved in CH_2Cl_2 (50 ml, 3.2×10^{-4} M). To this solution, ethylenediamine (0.15 M solution in methanol, 0.10 ml) was added. The solution was stirred at room temperature over 1 week. The conversion was monitored with TLC (silica gel, CH_2Cl_2–10% ether). Evaporation of the solvent and subsequent recrystallization (CH_2Cl_2–methanol) gave the porphyrin **1a** as purple crystals (10.0 mg, 0.011 mmol, 70%). ^1H NMR ($CDCl_3$) δ=12.47 (2H, br, OH), 10.08+10.06 (2H+2H, s+s, *meso*-H), 6.25 (2H, s, CH=N), 6.35+6.31+5.39 (each 2H, dd+d+d, Ar-H), 4.5+4.2 (2H+2H, m+m, β-$C\underline{H}_2CH_2CO$), 4.14—3.97(8H, m, β-$C\underline{H}_2CH_3$, OCH_2), 3.59+3.58 (6H+6H, s+s, β-CH_3), 3.3+3.1 (2H+2H, m+m, β-$CH_2C\underline{H}_2CO$), 2.84+2.16+2.06 (2H+2H+4H, m, CH_2-N=C, $OCH_2C\underline{H}_2$), 1.86 (6H, t, β-$CH_2C\underline{H}_3$), −3.74 (2H, br, NH). UV-Vis (CH_2Cl_2) 400, 498, 534, 568, and 621 nm. IR(KBr) 1730(C=O) and 1630 cm^{-1} (C=N). MS(FAB) *m/z* 887(M+H$^+$). Found: C, 72.36; H, 6.69; N, 9.04%. Calcd for $C_{54}H_{58}N_6O$: C, 73.11; H, 6.59; N, 9.48%.

3,3′-[Ethylenebis[(nitrilomethylidyne)(4-hydroxy-3,1-phenylene)]bis[1-propanol]Diester of Mesoporphyrin II (Salen-Capped Porphyrin 2a, SCP-3-H$_4$). From the bis(salicylaldehyde)-linked porphyrin **15** (20.4 mg, 0.023 mmol, in CH_2Cl_2 180 ml, 1.3×10^{-4} M), the salen-capped porphyrin **2a** was synthesized by the same procedure as described above to give purple crystals (17.0 mg, 0.019 mmol, 81%). ^1H NMR ($CDCl_3$) δ=12.5 (2H, br, OH), 10.04+10.02 (2H+2H, s+s, *meso*-H), 7.21 (2H, s, CH=N), 5.95+5.84+5.65 (each 2H, d+d+dd, Ar-H), 4.33 (4H, t, β-$C\underline{H}_2CH_2CO$), 4.05 (4H, m, β-$C\underline{H}_2CH_3$), 3.91 (4H, m, OCH_2), 3.63+3.59 (6H+6H, s+s, β-CH_3), 3.27 (4H, s, CH_2-N=C), 3.23 (4H, t, β-$CH_2C\underline{H}_2CO$), 1.81 (6H, t, β-$CH_2C\underline{H}_3$), 1.58+1.27 (4H+4H, t+m, OCH_2-$C\underline{H}_2C\underline{H}_2Ar$), −3.80 (2H, br, NH). UV-Vis (CH_2Cl_2) 400, 499, 533, 537, and 621 nm. IR(KBr) 1730(C=O) and 1630 cm^{-1} (C=N). MS(FAB) *m/z* 915 (M+H$^+$).

5,15-Bis(2-methoxycarbonylphenyl)-2,8,12,18-tetranethyl-3,7,13,17-tetramethylporphyrin (19).[4a,10] Bis(3-ethyl-4-methyl-2-pyrryl)methane[19] (2.2 g, 9.6 mmol) and methyl 2-formylbenzoate (1.6 g, 9.7 mmol) were dissolved in dry acetonitrile (120 ml) and trichloroacetic acid (0.3 g, 1.8 mmol) was added. The mixture was stirred at room temperature for 5 h and chloranil (4.5 g, 18 mmol) in dry THF (100 ml) was added. Stirring was continued overnight and solvent was evaporated. The residue was washed with water and with methanol. Recrystallization from CH_2Cl_2–methanol gave purple crystals (2.0 g, 56%). Second crops were obtained as zinc complexes from methanol filtrate after treating with zinc acetate (0.80 g, 21%). ^1H NMR ($CDCl_3$) δ=10.18 (2H, s, *meso*-H), 8.35+8.01+7.89+7.84 (each 2H, dd+dd+m+m, Ar-H), 4.00 (8H, m, β-$C\underline{H}_2CH_3$), 2.75 (6H, s, OCH_3), 2.43 (12H, s, β-CH_3), 1.76 (12H, t, β-$CH_2C\underline{H}_3$), −2.24 (2H, br, NH). MS(FAB) *m/z* 747 (M+H$^+$). Found: C, 76.55; H, 6.70; N, 7.28%. Calcd for $C_{48}H_{50}N_4O_4$: C, 77.18; H, 6.75; N, 7.50%.

5,15-Bis(2-carboxyphenyl)etioporphyrin II (20). 5,15-Bis-(2-methoxycarbonylphenyl)etioporphyrin II (**19**) (0.70 g, 0.94 mmol) was dissolved in pyridine (75 ml), water (20 ml), and methanol (20 ml) containing potassium hydroxide (5.4 g). This mixture was refluxed for 3 days in the dark and then poured into water and acidified with hydrochloric acid. The porphyrin was extracted with $CHCl_3$ and the organic layer was washed with water and evaporated. Recrystallization from pyridine–methanol gave purple crystals (0.48 g, 71%). MS(FAB) *m/z* 719 ($M+H^+$).

***cis*-5,15-Bis[2-(4-formyl-3-hydroxyphenoxycarbonyl)-phenyl]etioporphyrin II (6a:α,α).** 5,15-Bis(2-carboxyphenyl)etioporphyrin II (**20**) (97 mg, 0.135 mmol, the mixture of atropisomers was used without separation) was treated with oxalyl dichloride (1.0 ml) in CH_2Cl_2 by the same procedure as **4** to give porphyrin bis(acid chloride). 2,4-Dihydroxybenzaldehyde (0.50 g, 3.6 mmol) was suspended in dry CH_2Cl_2 (10 ml) and addition of pyridine (0.5 ml) gave clear solution. This solution was added to the solution of porphyrin bis(acid chloride) in CH_2Cl_2. The same work up procedure as **4** was carried out to give purple crystals of **6a** as isomers mixture (107.5 mg, 0.112 mmol 83%, α,α/α,β=1/3).

This mixture was separated by flash column chromatography on silica gel eluted with CH_2Cl_2–1% ether. The more polar compound was assigned as the *cis*-isomer **6a**: α,α (25 mg, 0.026 mmol, 19%).

^1H NMR ($CDCl_3$) δ=10.52 (2H, br, OH), 10.15 (2H, s, *meso*-H), 9.09 (2H, s, CHO), 8.49+8.09+7.9 (2H+2H+4H, m, *meso*-ArH), 6.33+5.82+4.97 (each 2H, d+d+dd, CO_2-ArH), 3.98 (8H, m, β-C<u>H</u>$_2$CH$_3$), 2.47 (12H, s, β-CH_3), 1.74 (12H, t, β-CH_2C<u>H</u>$_3$), −2.30 (2H, br, NH). UV-Vis (CH_2Cl_2) 412, 508, 541, 577, 653 nm. IR(KBr) 1730 and 1655 cm^{-1} (C=O). MS(FAB) *m/z* 959 ($M+H^+$).

Zinc 5,15-Bis[2-(4-formyl-3-hydroxyphenoxycarbonyl)-phenyl]etioporphyrin II (6c: α,α and 6c: α,β). *trans*-5,15-Bis[2-(4-formyl-3-hydroxyphenoxycarbonyl)phenyl]etioporphyrin II (**6a**: α,β) (150 mg) was converted to the zinc complexes and dissolved in *o*-dichlorobenzene (30 ml). The solution was refluxed for 24 h and then solvent was removed under reduced pressure. The *cis* and the *trans* isomer were easily separated by flash column chromatography eluted with CH_2Cl_2. The *trans* isomer **6c**: α,β (84.3 mg, 53%) was eluted first, followed by the *cis* isomer **6c**: α,α (50.5 mg, 32%). ^1H NMR ($CDCl_3$) δ=10.30 (2H, br, OH), 10.09 (2H, s, *meso*-H), 8.89 (2H, s, CHO), 8.46+8.13+7.94 (2H+2H+4H, m, *meso*-Ar-H), 6.32+5.55+5.13 (each 2H, d+d+dd, CO_2-Ar-H), 3.96 (8H, s, β-C<u>H</u>$_2$CH$_3$), 2.43 (12H, s, β-CH_3), 1.73 (12H, t, β-CH_2C<u>H</u>$_3$). Found: C, 69.76; H, 4.96; N, 5.42%. Calcd for $C_{60}H_{52}N_4O_8Zn$: C, 70.48; H, 5.13; N, 5.48%.

6c: α,β: ^1H NMR ($CDCl_3$) δ=10.39 (2H, br, OH), 10.12 (2H, s, *meso*-H), 9.07 (2H, s, CHO), 8.46+8.15+8.0 (2H+2H+4H, m, *meso*-Ar-H), 6.34+5.52+4.97 (each 2H, d+d+dd, CO_2–Ar–H), 3.97 (8H, s, β-C<u>H</u>$_2$CH$_3$), 2.44 (12H, s, β-CH_2), 1.74 (12H, t, β-CH_2C<u>H</u>$_3$).

Salen-Capped Porphyrin 3a, (SCP-*o*-H_4). The bis(salicylaldehyde)-linked porphyrin **6a**: α,α (8.3 mg, 0.0087 mmol, in CH_2Cl_2 50 ml, 1.7×10^{-4} M) was treated with ethylenediamine (0.15 M solution in methanl, 0.065 ml) by the same procedure as **1a** to give purple crystals (6.4 mg, 75%).

^1H NMR ($CDCl_3$) δ=10.17 (2H, s, *meso*-H), 8.43+8.17+7.9 (2H+2H+4H, m, *meso*-Ar-H), 7.26 (2H, s, CH=N), 5.71+5.67+4.16 (each 2H, d+d+dd, CO_2-Ar-H), 4.01 (8H, m, β-C<u>H</u>$_2$CH$_3$), 3.42 (4H, s, CH_2–N=C), 2.49 (12H, s, β-CH_3), 1.77 (12H, t, β-CH_2C<u>H</u>$_3$), −2.41 (2H, br, NH). UV-Vis (CH_2Cl_2) 412, 508, 541, 577, 625, 656 nm. IR(KBr) 1725(C=O) and 1625 cm^{-1} (C=N). MS(FAB) *m/z* 983 ($M+H^+$).

Salen-Capped Porphyrin 3c, (SCP-*o*-H_2Zn). The zinc bis(salicylaldehyde)-linked porphyrin **6c**: α,α (49 mg, 0.048 mmol, in CH_2Cl_2 300 ml, 1.6×10^{-3} M) was treated with ethylenediamine (0.15 M solution in methanol, 0.35 ml) by the same procedure as **1a** to give purple crystals (40 mg, 80%).

^1H NMR ($CDCl_3$) δ=10.08 (2H, s, *meso*-H), 8.40+8.03+7.93+7.85 (each 2H, d+d+m+m, *meso*-Ar-H), 7.32 (2H, s, CH=N), 5.94+5.03+4.77 (each 2H, d+s+d, CO_2-Ar-H), 3.97 (8H, m, β-C<u>H</u>$_2$CH$_3$), 3.37 (4H, s, CH_2–N=C), 2.45 (12H, s, β-CH_3), 1.76 (12H, t, β-CH_2C<u>H</u>$_3$). UV-Vis (CH_2Cl_2) 417, 543, 583 nm.

General Metallation Procedure: Nickel. Solution of nickel(II) acetate in methanol was added to the salen-capped porphyrin dissolved in CH_2Cl_2. The mixture was stirred for about 5 h at room temperature and then the solvent was evaporated. Recrystallization from CH_2Cl_2–methanol or from CH_2Cl_2–hexane gave the corresponding nickel-salen complexes.

Zinc. A saturated solution of zinc acetate in methanol was added to the porphyrin dissolved in CH_2Cl_2. The mixture was stirred at room temperature for 1 h. The solvent was removed and the residue was washed with water and then recrystallized from CH_2Cl_2–methanol or from CH_2Cl_2–hexane to give zinc-porphyrin complexes.

1b: ^1H NMR ($CDCl_3$) All signals were broad and poorly resolved, δ=9.90+9.84 (2H+2H, *meso*-H), 7.09+6.87+6.39 (each 2H, Ar-H or CH=N), −1.42+−1.72 (4H, CH_2–N=C), −3.73 (2H, NH). UV-Vis (CH_2Cl_2) 403, 504, 538, 568, 621 nm. MS(FAB) *m/z* 943—946 ($M+H^+$).

1c: ^1H NMR ($CDCl_3$) δ=11.11 (2H, br, NH), 9.94+9.88 (each 2H, s, *meso*-H), 6.46 (2H, s, CH=N), 6.24+5.65+4.90 (each 2H, dd+d+d,Ar-H), 4.48+4.1 (12H, m, β-CH_2, OCH_2), 3.57+3.54 (6H+6H, s+s, β-CH_3), 3.34+3.15 (2H+2H, m, β-CH_2C<u>H</u>$_2$CO), 2.78+2.67 (4H, m, CH_2–N=C), 2.22+2.16 (2H+2H, m, OCH_2C<u>H</u>$_2$Ar), 1.86 (6H, t, β-CH_2-C<u>H</u>$_3$), UV-Vis (CH_2Cl_2) 404, 536, 572 nm. MS(FAB) *m/z* 949—952 ($M+H^+$).

1d: ^1H NMR ($CDCl_3$) δ=9.95+9.88 (each 2H, s, *meso*-H), 6.71+6.20+5.80 (each 2H, br, Ar-H or CH=N), the other signals were not assigned. UV-Vis (CH_2Cl_2) 410, 538, 574 nm. MS(FAB) *m/z* 1004—1012 (M^+).

2b: UV-Vis (CH_2Cl_2) 402, 502, 536, 569, 624 nm.

2d: ^1H NMR ($CDCl_3$) δ=10.20+9.96 (2H+2H, s+s, *meso*-H), 5.88+5.78+4.67 (each 2H, dd+d+d, Ar-H), 5.52 (2H, s, CH=N), 4.22+4.05 (12H, m, β-CH_2, OCH_2), 3.66+3.64 (6H+6H, s+s, β-CH_3), 3.23+3.12 (4H, m, β-CH_2C<u>H</u>$_2$CO), 2.54 (4H, m, CH_2–N=C), 1.89 (6H, t, β-CH_2CH_3). UV-Vis (CH_2Cl_2) 404, 535, 571 nm. MS(FAB) *m/z* 1032—1038 (M^+).

3b: ^1H NMR ($CDCl_3$) All signals were broad, δ=10.17+10.01 (1H+1H, *meso*-H), 8.02+7.87+7.71 (8H, *meso*-Ar-H), 5.76+4.56+3.87 (16H, CO_2-Ar-H, β-C<u>H</u>$_2$CH$_3$), 2.49+2.43 (6H+6H, β-CH_3), 1.57 (12H, β-CH_2C<u>H</u>$_3$), −1.38 (4H, CH_2–N=C), −2.40 (2H, NH). UV-Vis (CH_2Cl_2) 406, 505, 539, 572, 624, 654 nm. IR (KBr) 1730 (C=O) and 1610 cm^{-1} (C=N).

3d: ^1H NMR ($CDCl_3$) δ=9.94 (2H, s, *meso*-H), 8.05+7.84+7.64+7.50 (each 2H, m+t+t+d, *meso*-Ar-H), 5.99+5.76+4.84 (each 2H, br, CO_2-Ar-H), 3.9—3.7 (12H, m, β-C<u>H</u>$_2$CH$_3$, CH_2–N=C), 2.41 (12H, s, β-CH_3), 1.59 (12H, t,

β-$CH_2C\underline{H}_3$). UV-Vis (CH_2Cl_2) 418, 548, 583 nm. MS(FAB) *m/z* 1100—1106(M^+).

Strapped Porphyrin 21.[20] **21a**: ^{1}H NMR ($CDCl_3$) δ=10.16 (2H, s, *meso*-H), 8.37+7.8 (8H, m, Ar-H), 3.99 (8H, m, β-$C\underline{H}_2CH_3$), 3.31 (4H, t, OCH_2), 2.45 (12H, s, β-CH_3), 1.77 (12H, t, β-$CH_2C\underline{H}_3$), −0.28+−0.83+−1.05+−1.18 (each 4H, m+m+br+br, $OCH_2(C\underline{H}_2)_8CH_2O$), −2.19 (2H, br, NH). UV-Vis (CH_2Cl_2) 411, 509, 541, 580, 629 nm. MS(FAB) *m/z* 857 ($M+H^+$).

21c: ^{1}H NMR ($CDCl_3$) δ=10.13 (2H, s, *meso*-H), 8.33+7.83 (8H, m, Ar-H), 3.98 (8H, m, β-$C\underline{H}_2CH_3$), 3.26 (4H, t, OCH_2), 2.42 (12H, s, β-CH_3), 1.76 (12H, t, β-$CH_2C\underline{H}_3$), −0.29+−0.73+−0.93+−1.01 (each 4H, m+m+br+br, $OCH_2(C\underline{H}_2)_8CH_2O$). UV-Vis ($CH_2Cl_2$) 413, 540 and 575 nm. MS(FAB) *m/z* 918—923 (M^+).

This work was supported by a Grant-in-Aid for Special Project Research No. 63104003 from the Ministry of Education, Science and Culture and by Mitsubishi Foundation for Scientific Research. We thank Professor Satoshi Hirayama of Kyoto Institute of Technology for measurement of picosecond fluorescence lifetimes. We also thank Professor Noboru Mataga of Osaka University for measurement of time-resolved absorption spectra.

References

1) D. E. Fenton, "Do Binucleating Ligands have a Biological Relevance?" in "Advances in Inorganic and Bioinorganic Mechanisms," ed by A. G. Sykes, Acad. Press, New York (1983), Vol. 2, pp. 187—257.

2) D. Dolphin, J. Hiom, and J. B. Paine III, *Heterocycles*, **16**, 417 (1981); S. S. Eaton, G. R. Eaton, and C. K. Chang, *J. Am. Chem. Soc*, **107**, 3177 (1985); J. L. Sessler, M. R. Johnson, T. Y. Lin, and S. E. Creager, *J. Am. Chem. Soc*, **110**,3659 (1988); A. Osuka and K. Maruyama, *J. Am. Chem. Soc.*, **110**, 4454 (1988) and references cited in these publications.

3) C.K.Chang, *J. Am. Chem. Soc.*, **99** , 2819 (1977); N. M. Richardson, I. O. Sutherland, P. Camilleri, and J. A. Page, *Tetrahedron Lett.*, **1985**, 3739; V. Krishnan, *J. Am. Chem. Soc.*, **104**, 3463 (1982); A. Hamilton and J. M. Lehn, *ibid.*, **108**, 5158 (1986).

4) a) M. J. Gunter and L. N. Mander, *J. Org. Chem.*, **46**, 4792 (1981); b) D. A. Buckingham, M. J. Gunter, and L. N. Mander, *J. Am. Chem. Soc.*, **100**, 2899 (1978); c) C. K. Chang, M. S. Koo, and B. Ward., *J. Chem. Soc., Chem. Commun.*, **1982**, 716; d) N. G. Larsen, P. D. W. Boyd, S. J. Rodgers, G. E. Wuenschell, C. A. Koch, S. Rasmussen, J. R. Tate, B. S. Erler, and C. A. Reed, *J. Am. Chem. Soc.*, **108**, 6950 (1986).

5) Preliminaly report of this work has published: K. Maruyama, F. Kobayashi, and A. Osuka,*Chem. Lett.*, **1987**, 821.

6) J. P. Collman, P. Denisevich, Y. Konai, M. Marrocco, C. Koval, and F. C. Anson, *J. Am. Chem. Soc.*, **102**, 6027 (1980).

7) K. N. Ganesh and J. K. M. Sanders, *J. Chem. Soc., Perkin Trans. 1*, **1982**, 1611.

8) G. Casraghi, G. Casnati, G. Puglia, G. Sartori, and G. Terenghi, *J. Chem. Soc., Perkin Trans. 1*, **1980**, 1862.

9) Reversible Schiff base formation was once used in the synthesis of a quinone-capped porphyrin: J. S. Lindsey and D. C. Mauzerall, *J. Am. Chem. Soc.*, **104**, 4498 (1982).

10) R. Young and C. K. Chang, *J. Am. Chem. Soc.*, **107**, 898 (1985); K. Maruyama, T. Nagata, F. Kobayashi, A. Osuka, *J. Hetrocycl. Chem.*, in press.

11) K.N.Ganesh and J. K. M. Sanders, *J. Chem. Soc., Chem. Commun.*, **1980**, 1129; K. N. Ganesh, J. K. M. Sanders, and J. C. Waterton, *J. Chem. Soc., Perkin Trans. 1*, **1982**, 1617.

12) L. M. Schol'nikova, E. M. Yumal', E. A. Shugam, and V. A. Voblikova, *J. Struct. Chem. (Engl. Transl.)*, **11**, 819 (1970).

13) On heating the solution of **3b** in $CDCl_3$, two sets of signals became closer but were not completely merged at 41 °C.

14) R. J. Abraham, S. C. M. Fell, and K. M. Smith, *Org. Magn. Reson.*, **9**, 367 (1977).

15) H. Ohya, *Bull. Chem. Soc. Jpn.*, **52**, 2064 (1979).

16) M. Nappa and J. S. Valentine, *J. Am. Chem. Soc.*, **100**, 5075 (1978).

17) S. Hirayama and Y. Shimoto, *J. Chem. Soc., Faraday Trans. 2*, **80**, 941 (1984).

18) H. Miyasaka, H. Masuhara, and N. Mataga, *Laser Chem.*, **1**, 357 (1983).

19) P. S. Clezy and A. W. Nichol, *Aust. J. Chem.*, **11**, 1835 (1965).

20) Strapped porphyrin **21a** was synthesized directly from bis(3-ethyl-4-methyl-2-pyrryl)methane and 1,10-decanediol bis(2-formylbenzoate): A. Osuka, F. Kobayashi, T. Nagata, and K. Maruyma, *Chem. Lett.*, **1990**, 287.